Numerical Simulation of High-Speed Joining

Prof. Dr.-Ing. Gerson Meschut, Dipl.-Ing. Michael Gerkens

Laboratory for material and joining technology (LWF®), Paderborn University

1 Introduction

Structures made of sheet metal profiles place stringent demands on joining technology due to the combination of high-strength and ultra-high strength steels and extruded aluminium profiles involved. Apart from the requirement for accessibility from one side, it is also necessary to avoid deformation of the parts. High-speed tack setting (High-Speed Joining) only requires accessibility from one side and is performed without any pre-punching operations. During joining, the inertia of the component is exploited, which means that no further tools are required. The high joining speeds of up to 40 m/s permit a process time of less than a second, making the process economically attractive. High-speed tack setting also offers a high degree of flexibility. Employing a tack-setting geometry, it is possible to join a big range of sheet thicknesses, achieve two or multiple-sheet joints, and join highly different materials, without needing to change ancillary parts or joining tools. It is also feasible for the tack setting tool to be applied to an industrial robot [1]. One challenge is the high process dynamics with the accompanying acoustic burden. The local stiffness is also of prime importance. Numerical simulation is a suitable tool for estimating joinability and load-bearing capacity. Two-dimensional simulations are particularly appropriate for depicting rotationally symmetric joining processes, such as for laboratory specimens with die support. For depicting non-symmetrical situations, by contrast, it is essential to use of 3D simulations. The results set out below were generated at the LWF® in the course of IGF Project 17893 N.

2 Process description

High-speed tack setting is based on the push-rod principle. A driving piston is pneumatically accelerated and drives the tack into the parts to be joined. As the tack enters the metal sheet, most of the kinetic energy is converted into mechanical work or heat. The remaining surplus energy is absorbed by a rubber bump stop. A diagram of the tack-setting tool is shown on the left of Fig. 1 and the individual process stages on the right.

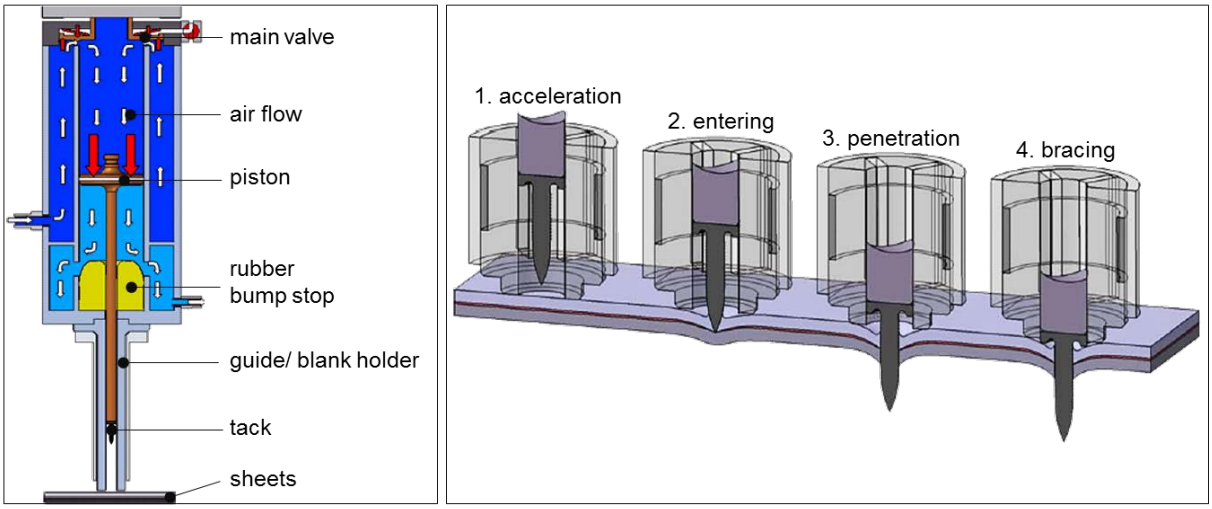

Fig.1: Left: The layout of the tack-setting tool [2], right: The stages of the joining process [3]

1. Acceleration phase: The blank holder is positioned on the sheets to be joined with a defined force and holds them in place. The driving piston is pneumatically accelerated and drives the tack. The tack is guided through the blank holder. The set pressure is the control parameter.

2. Entering phase: The ogival tip of the tack enters the sheets and displaces the material in the radial direction, and also counter to the joining direction. Inertia effects and the local stiffness of the part are exploited here.
3. Penetration phase: The tip of the tack penetrates the sheets in their entirety, so that the profiled tack shaft can achieve both a force and a form fit with the hole it has made. The deformation and friction work required for this leads to a high level of local heating, promoting the flow properties of the materials.
4. Bracing phase: The surplus kinetic energy is absorbed when the piston strikes the rubber bump stop, or is converted into reversible spring energy in the sheet metal. The mouthpiece removes the load from the joined sheets.

High-speed tack setting is based primarily on force and form-fit retaining mechanisms. Earlier studies, however, have also described cold welds and a material bond, which are indications of the high process temperatures that develop at the point where the tack enters the sheet [4]. These temperature effects and the high process speeds, with the resulting high strain rates, place stringent requirements on the simulation.

3 Material description

3.1 Plasticity

3.1.1 Johnson-Cook model

Two materials were investigated by way of example: a micro-alloyed flat steel, HC340LAD, and an aluminium profile material, EN AW6060-T66. Since the joining process is highly dynamic and local heat arises in the entry zone, it is necessary to have a strain-rate and temperature-dependent description of the material. The Johnson-Cook thermo-viscoplastic material model is suitable for this. The main advantage of this material model is its multiplication approach, i.e. the strain rates and temperature effects can be described independently of each other. The “adiabatic” heating through plastic deformation is described by the Taylor-Quinney coefficient (parameter BETA or XS1) and does not require any thermal coupling. Each element heats up individually as a result of its deformation.

First of all, use was made of the material model ***MAT107(*MAT_MODIFIED_JOHNSON_COOK)**, cf. [5], where the plasticity and the failure are defined on the basis of parameters. Formula (1) shows the Johnson-Cook plasticity with the Ludwik formulation and formula (2) the calculation of the homologous temperature.

$$\sigma_F = \left(A + B \cdot \varepsilon_v^{pl\,n}\right) \cdot \left(1 + \frac{\dot{\varepsilon}_v^{pl}}{\dot{\varepsilon}^0}\right)^C \cdot \left(1 - T^{*m}\right) \tag{1}$$

where

$$T^* = \frac{T - T_R}{T_m - T_R} \tag{2}$$

The material model ***MAT224(*MAT_TABULATED_JOHNSON_COOK)** additionally offers greater flexibility in describing the flow curve and the damage curve. It is possible to define temperature-dependent moduli of elasticity, as well as temperature and strain-rate dependent heat development and correlations with the element size for the failure description. In older solvers, there were problems with the implicit springback simulation and with the definition of a temperature-dependent modulus of elasticity. These and other problems have now been eliminated as of Version R9.0.1, see [6].

3.1.2 Experimental investigations

Experimental investigations were conducted on the materials in tensile tests at strain rates qs of 1, 10, 100 and 500 1/s and temperatures of 20, 100, 200 °C. The flow curves for HC340 were extrapolated according to Ludwik and those for EN AW6060 according to Voce. The experimental results are shown on representative curves in the following Figure.

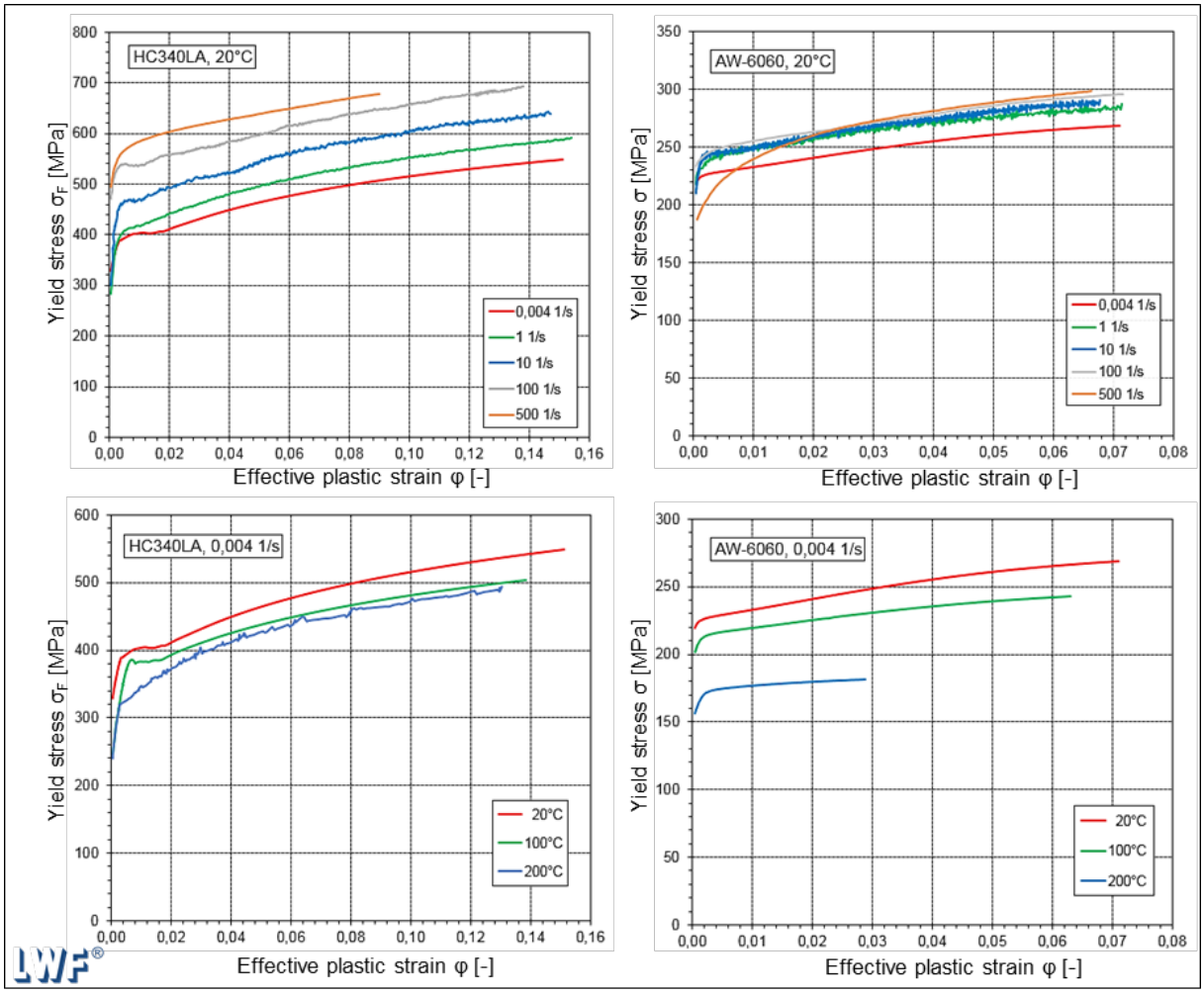

Fig.2: Experimentally determined flow curves for materials HC340LA (left) and EN AW6060-T66 (right) for different strain rates and temperatures

3.2 Damage modelling

To depict the penetration and tearing open of the sheet metal in the simulation, use was first made of the Johnson-Cook damage model ***MAT107**. This describes a failure strain as a function of the triaxiality by means of an exponential formulation. Taking the HC340LAD as an example, the necessary damage specimens were investigated experimentally and simulated, and quasi-static, isothermal damage parameters (D_1 to D_3) were identified. The following formula (3) shows the calculation for the failure strain; a correlation with the triaxiality exists here, see formula (4).

$$\varepsilon_f = \left(D_1 + D_2 \cdot e^{D_3 \cdot \sigma^*}\right) \cdot \left(1 + \frac{\dot{\varepsilon}_v^{pl}}{\dot{\varepsilon}^0}\right)^{D_4} \cdot \left(1 + D_5 T^*\right) \tag{3}$$

where

$$\sigma^* = \frac{\sigma_m}{\sigma_v} \tag{4}$$

The plasticity parameters A, B, n and the damage parameters D_1 to D_3 were identified with the aid of an optimisation strategy in LS-Opt, employing different specimen geometries. It was possible to considerably delimit the flow properties beforehand by means of a simulation. Figure 3 below shows a comparison of the experimental and simulated force-displacement curves and also the derived failure curves as a function of the triaxiality.

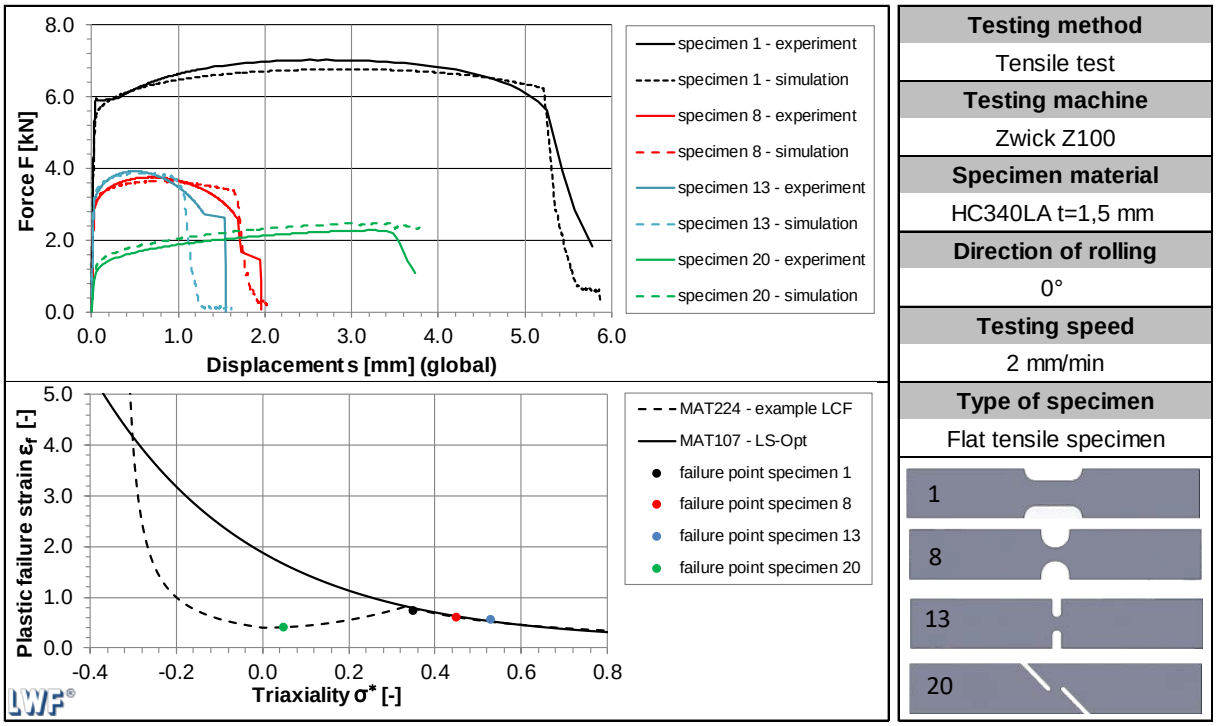

Fig.3: Top: Force-displacement curve for the damage specimens in the experiments and the simulation, bottom: Failure curve to Johnson-Cook with specimen failure points marked

The modelling of damage is a highly complex subject. The use of an exponential function to describe the elongation at break in ***MAT107** means that no unsteadiness can be depicted on purely mathematical grounds, and hence the shear and compression failure are inadequately assessed in the investigations conducted. Two-axis stress states ($\sigma^* > 0$), by contrast, can be readily depicted by the Johnson-Cook model. Preliminary work has revealed more of a garland-like profile for the failure strain, which is marked in with a dotted line on Fig. 3. An overview of current damage models, including Johnson-Cook, Cockroft-Latham and also forming limit diagrams (FLD) can be found in [7].
In order to nonetheless try out the Johnson-Cook model, damage parameters D_1 to D_3 were identified without consideration to the shear specimens. Material ***MAT224** makes it possible to save any desired failure curve over parameter LCF. In addition, the elongation at break can also be defined as a function of the lode angle parameter, by dafining a table for LCF. Detailed damage investigations may be found in [8] and the GISSMO model in LS-Dyna [9].
In both the 2D and the 3D simulations, the deletion of the elements when the failure strain is attained leads to a high-volume loss, which has a negative effect on the calculation of the contact forces. For this reason, the damage formulation to Johnson-Cook was not used any further for the 2D simulations. Instead, remeshing algorithms per ***Control_adaptive** were used.

4 2D simulations

Two-dimensional, rotationally symmetric models were compiled for simulating the joining process and the load-bearing capacity during pullout. Influential boundary conditions were identified through various sensitivity investigations. In the process and load-bearing-capacity simulations, two-sheet joints in steel and aluminium, with sheet thicknesses of 1.5 to 3.0 mm, were depicted. In addition, simulations were compiled for material characterisation, the depiction of system components (e.g. rubber bump stop) and for establishing the component stiffness. Selected simulation models and results will be presented in what follows.

4.1 Simulation of the joining process

In the process simulation, it is possible to avoid the above-mentioned problems relating to damage through ingenious remeshing. The tack was first depicted as rigid and without any profiling. As the next step, the flow curves of the tack material and the detailed profile geometry were determined. The tack was thus depicted with material model ***MAT024** and with allowance for the profiling. Details of the model structure are shown in Fig. 4.

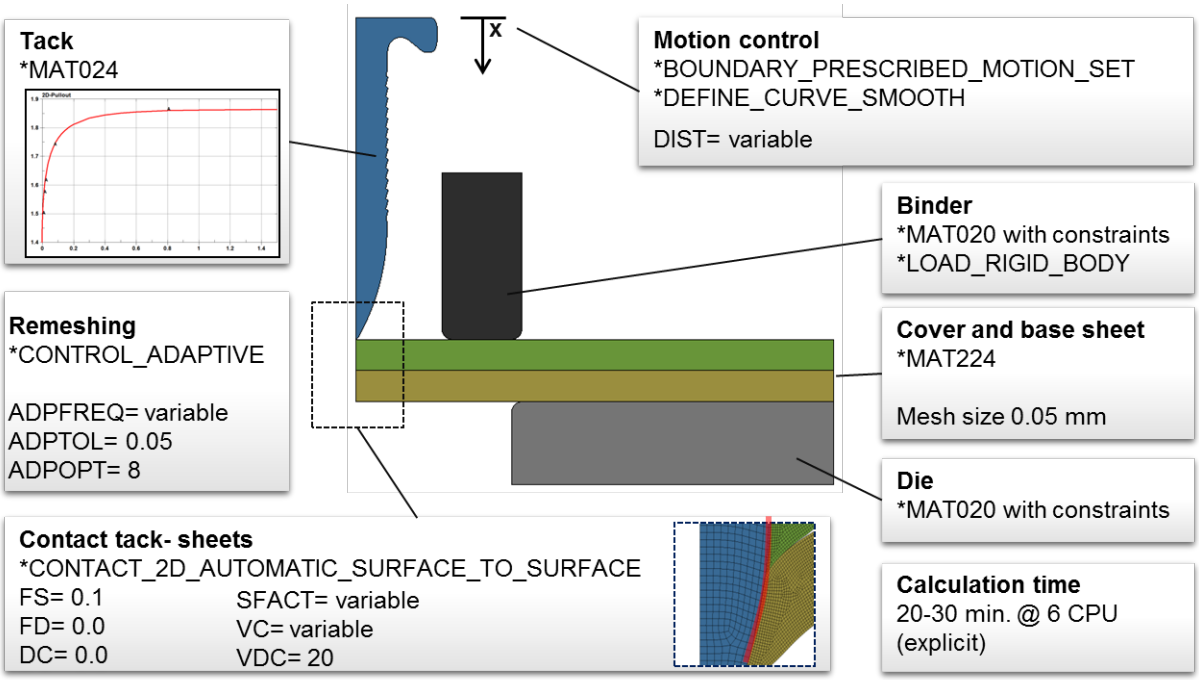

Fig.4: Model structure for simulation of the joining process (explicit) with downstream springback simulation (implicit)

As expected, making allowance for the profiling has a major influence on the form fit between the tack and the sheets, especially when ductile materials are being joined. The geometric depiction of the profiling, however, requires a very fine mesh with an element length of around 0.05 mm, and this necessitates a great deal of computing power, particularly for 3D simulations. The simulation of thermal effects, e.g. heat conversion from plastic work and friction, also shows clear effects in respect of flow properties. One challenge lies in finding the correct setting for the remeshing. If the frequency is too low (**ADPFREQ**) the mesh degenerates and the simulation breaks off. If the frequency is too high, non-physical effects, such as a thickening of the sheet, can occur.

4.2 Simulation of load-bearing capacity

The load-bearing capacity of the joint counter to the joining direction is depicted in a downstream pullout simulation. To do this, the cover sheet is cut by means of automated commands, and the simulation result for the process simulation, with allowance for the form and force fit, is transposed to the pullout simulation. This is done with the keyword ***INTERFACE_SPRINGBACK_LSDYNA**, which writes out the deformed mesh and the stress states. (***INITIAL_STRESS_SHELL**). Via ***INCLUDE** it is possible to import the mesh and the stress state into the pullout simulation. In this way, the effects from the process simulation can be taken into account in the load-bearing-capacity simulation. The detailed model structure is shown in Fig. 5.
When simulating pullout with steel sheet in the base layer, the force fit was seen to be decisive. To depict this, it is necessary to have a precise description of the friction as a function of the relative speed. In the case of the form fit, it was seen that soft aluminium, in particular, flows into the profiling during pullout. To depict the aluminium shear-off through the profiling that was observed in the experiments, further-reaching investigations would have to be carried out in respect of damage modelling. The softer the material, the more pronounced the form fit.

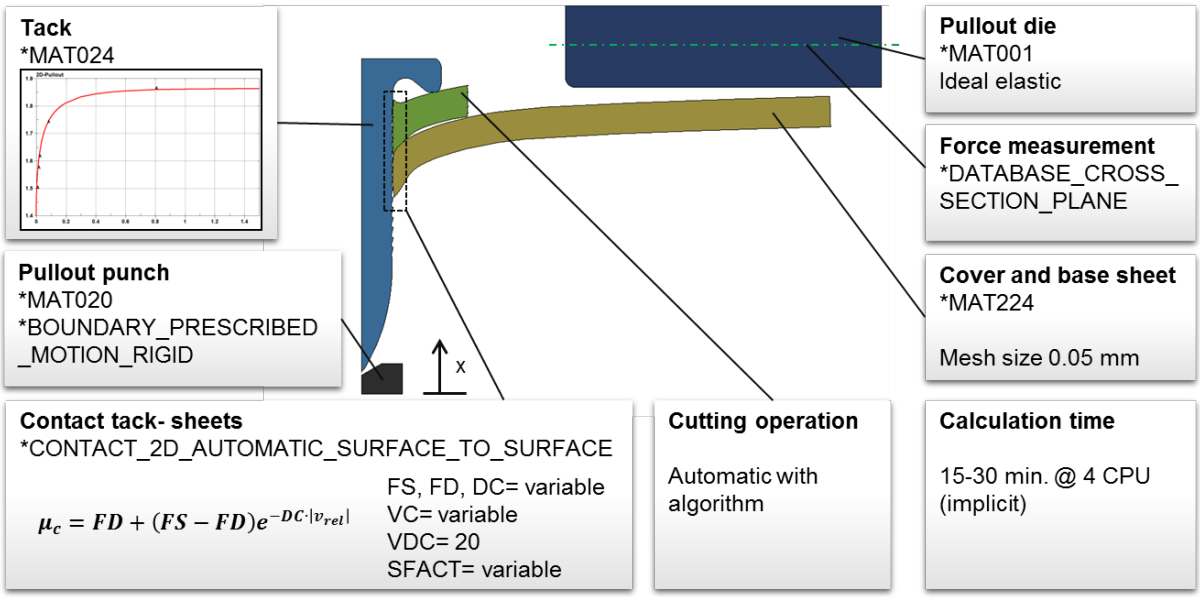

Fig.5: Model structure for the load-bearing-capacity simulations (implicit)

A large number of variants were derived from the models described above and sensitivities analysed. Hence, the tack was depicted both with and without profiling, and as rigid and elastic-plastic. In addition, the volume loss due to damage was determined. One question was also the extent to which thermal effects should be taken into account and what effect process control has in the simulation.

5 Simulation results

To validate the process simulation, geometric criteria such as the gap formation between the sheets being joined or the final position of the setting head are defined, cf. Fig. 6. The experimentally joined specimens were measured on polished microsections.

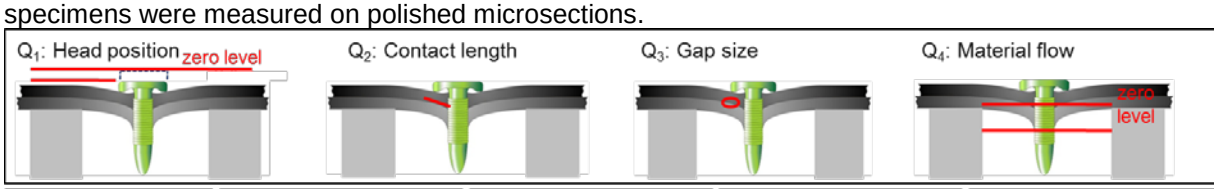

Cover sheet/ Base sheet	HC340LA 1,5/ HC340LA 1,5		HC340LA 2,0/ HC340LA 2,0		HC340LA 1,5/ EN AW-6060 3,0		EN AW-6060 2,0/ EN AW-6060 3,0	
	experiment	simulation	experiment	simulation	experiment	simulation	experiment	simulation
Q_1: Head position	0.63	0.71	0.48	0.50	0.21	0.49	0.35	0.13
Q_2: Contact length	0.71	0.72	0.71	0.74	1.36	1.22	1.64	1.33
Q_3: Gap size	0.23	0.15	0.31	0.22	0.26	0.07	0.25	0.12
Q_4: Material flow	2.69	2.80	2.40	2.60	2.81	2.58	2.36	2.33
Legend	difference < 20 %		difference 20-50 %		difference > 50 %			

Fig.6: Geometric assessment of the simulation results

The simulations for the steel combinations reveal good agreement with the experiment. The differences are greater when aluminium is used, however. The aluminium simulations are not so stable and require more remeshing steps, among other things. The modelling of the material and the friction model would seem to have an influence here.

Despite the geometric deviations and the model simplifications, meaningful pullout forces were obtained in overall terms, cf. Fig. 7. Making allowance for experimental scatter, the simulation depicts the maximum pullout force in a satisfactory manner.

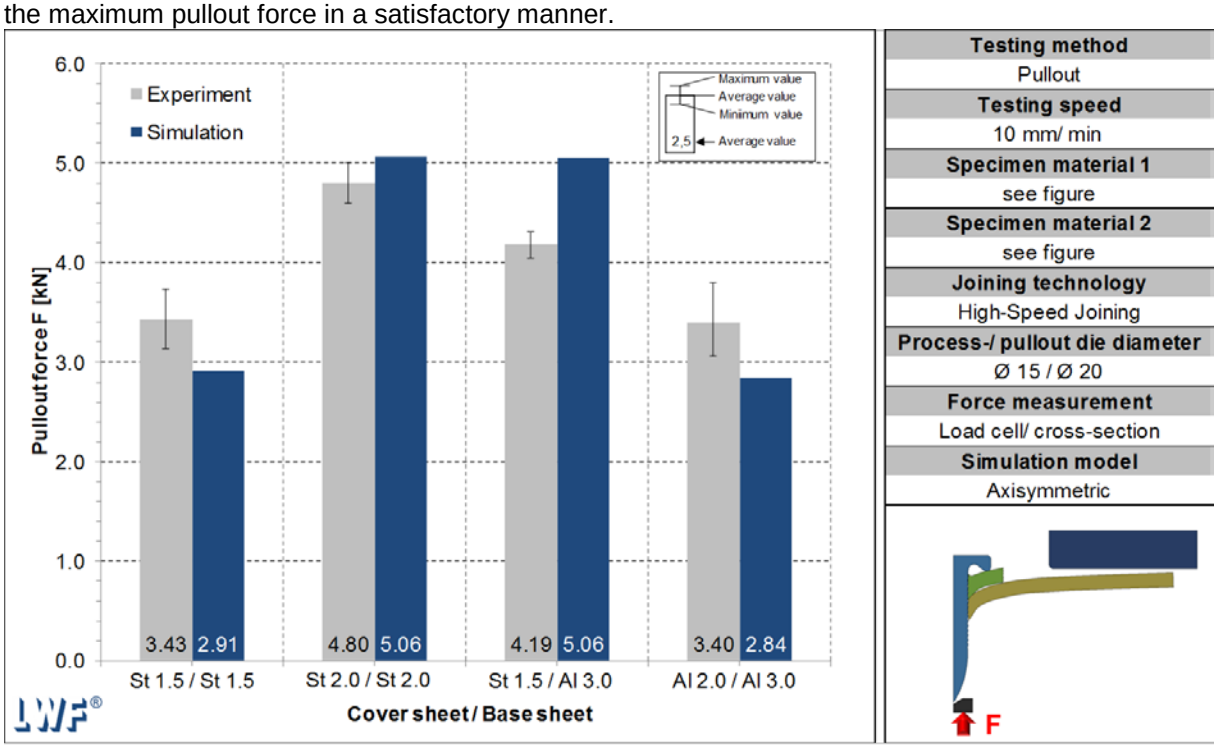

Fig.7: Experimentally determined and simulated pullout forces

The process simulations use a simple friction value model where only a static coefficient of friction FS and the viscous friction VC are set with parameter. For aluminium, VC = 100 was selected and, for steel, VC= 200. For the pullout simulation, by contrast, the following friction value formulation is used:

$$\mu_c = FD + (FS - FD) \cdot e^{-DC \cdot |v_{rel}|} \tag{5}$$

The transition from static adhesive friction to dynamic sliding friction is described by means of an exponential formulation. The friction values FS and FD were established for both materials at the LWF®. The relative speed for the determination of FD was approx. 130 mm/s, which is more than sufficient for the pullout simulation. The exponential decay coefficient DC was selected in such a way that $\mu_c(v_{rel}= 130) = FD$. In the simulations, it is seen that the maximum pullout force is generally only attained after the tack has started to “slide”. This is because, as the pullout displacement increases, the form fit between the base sheet and the tack profiling becomes more pronounced. Also, the deformation of the sheets in the joining process leads to a kind of self-reinforcement during pullout, which means that the gripping forces and hence the friction fit is increased. To isolate the influence of the friction value, pullout simulations were performed where only FS was varied. The same input data (**`*dynain`**) was always taken as a basis. The influence of the static friction is shown in Fig. 8.
As expected, the pullout force increases in an equivalent manner when the friction value rises. With friction values in excess of 0.25, no significant increase in the pullout force is evident any more. One explanation for this is that parameter VC is decisive here, or that it is primarily the deformation of the sheet metal that is measured.

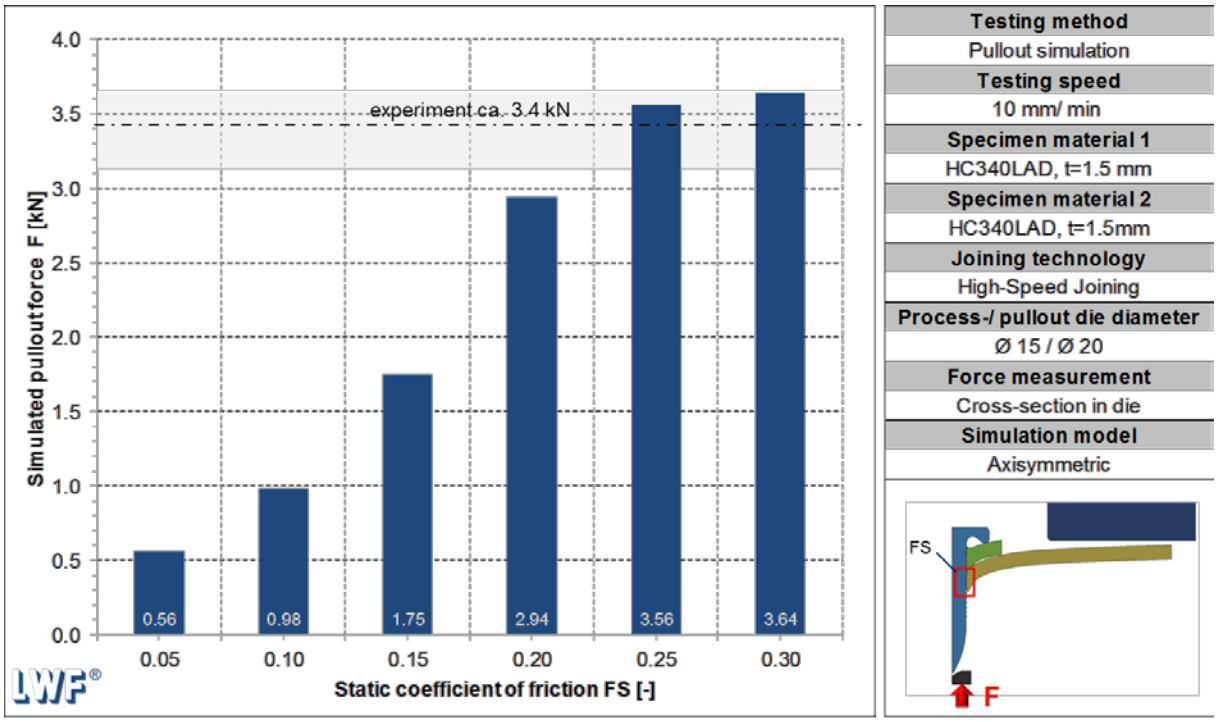

Fig.8: Simulated pullout forces as a function of the static coefficient of friction FS

If the joining pressure is set too high in high-speed tack setting, the head can hit the sheet too hard (puncture), which can lead to a reduction in load-bearing capacity. In the process simulation, the head impact was simulated through an increase in the tack displacement of 0.1 or 0.2 mm. Figure 9 shows that the puncture in the process simulation leads to a marked reduction in the pullout force, while a head protrusion (a 0.1 mm reduction in the displacement) has no negative impact.

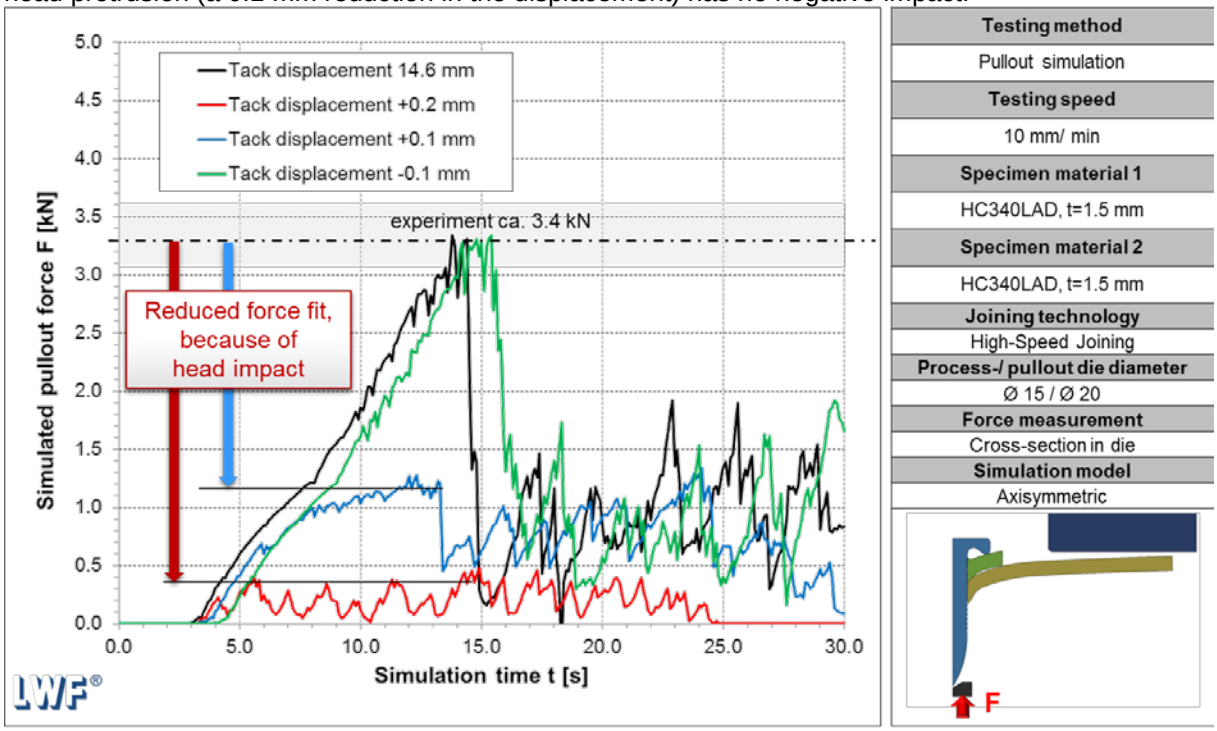

Fig.9: Simulated pullout force-displacement curve as a function of the tack displacement in the process simulation

The results show that, despite the simplified process control, a puncture can be depicted within the process simulation. It proved possible to obtain a large number of other detailed findings from the simulation which will not be gone into in greater depth here.

6 Summary

Using the simulations developed, it is possible to conduct detailed numerical process and load-bearing capacity analyses. The process simulations allow the prediction of the geometric formation, the joining energy required and the necessary piston displacement. Giving consideration to the system components of driving piston and elastomer stop, it is possible to estimate the necessary piston speed and system pressure. The simulations of the load-bearing capacity make it possible to predict the pullout forces, with allowance for the force-fit and form-fit retaining mechanisms. The simulations also show a direct correlation with the stiffness of the joining points.
Material characteristic values were established and corresponding material models defined (***MAT024, *MAT107, *MAT224**). To describe the sheets, strain rates of up to 500 1/s and temperatures of up to 200 °C were taken into account. For the steel, Johnson-Cook parameters were taken up by way of example and integrated in a damage model. The material parameters of the elastomer buffer and the tack were also characterised.
From the detailed simulations, it proved possible to gain new findings in respect of the local effects that take place during tack setting which are of relevance for understanding the process and determining the characteristic values. Describing the friction value constitutes a particular challenge. Further-reaching 3D simulations will be required for non-symmetrical load-bearing capacity investigations. These require a great deal of computing power on account of the fine mesh required (approx. 0.05 mm) to depict the form fit of the profiling. Further details of the simulation of high-speed tack setting may be found in the final report for the project mentioned.

7 Funding and acknowledgements

The presented IGF-project 17893N / EFB-project 02/211 of the European Research Association for Sheet Metal Working e.V. (EFB), Lothringer Str. 1, 30559 Hannover was funded by the AiF as part of the program for the promotion of Industrial Collective Research (IGF) by the Federal Ministry for Economic Affairs and Energy, based on a decision of the German Bundestag.
The research centers thank the above-mentioned institutions and the member companies of the project support committee for their promotion and support of the research project.

8 Literature

[1] Hahn, O.; Janzen, V.; Meschut, G.; Olfermann, T.; Süllentrop, S.: “Fügeverfahren in hybriden Leichtbausystemen”, ATZ/MTZ Fachbuch Leichtbau in der Fahrzeugtechnik, Wiesbaden, Springer-Vieweg, 2013, p. 638

[2] Möhring, J.: “Qualifizierung von Fügeelementbeschichtungen für den Einsatz des druckluftbetriebenen Bolzensetzens im Karosseriebau”, Dissertation, Universität Paderborn, 2011, p.32

[3] Kohl, D.: “Entwicklung und Qualifizierung eines Qualitätsprüfkonzeptes für das Hochgeschwindigkeits-Fügeverfahren Bolzensetzen im Automobil-Leichtbau”, Dissertation, Universität Paderborn, 2014, p.17

[4] Draht, T.: “Entwicklung des Bolzensetzens für Blech-Profil-Verbindungen im Fahrzeugbau”, Dissertation, Universität Paderborn, 2009, p. 21

[5] LS-Dyna Keyword Users’s Manual Volume II- Material Models, LS-Dyna R9.0, 31.08.2016, p. 598-605 and 1130-1135

[6] http://www.dynasupport.com/news/ls-dyna-r9.0.1-r9.109912-released, last called up on 24.03.2017

[7] Lee, Y.-W.: Fracture prediction in metal sheets, Dissertation, Massachusetts Institute of Technology, 2005, pp. 63-78

[8] Basaran, M.: “Stress State Dependent Damage Modeling with a Focus on the Lode Angle Influence”, Dissertation, Rheinisch-Westfälischen Technischen Hochschule Aachen, 2011, p. 98-104

[9] Basaran, M.; Wölkerlking, S. D.; Ferucht, M.; Neukamm, F.; Weichert, D.: “An Extension of the GISSMO Damage Model Based on Lode Angle Dependence”, paper on 9. LS-Dnya Anwernderforum Bamberg, 2010